Journal of Statistical Physics, Vol. 29, No. 3, 1982

Intersecting Disks (and Spheres) and Statistical Mechanics. II. The Hard-Disk System

Karl W. Kratky and Herbert Drexler[1]

Received November 4, 1981; revised May 20, 1982

A system of hard disks (diameter σ) is studied by considering the corresponding exclusion disks (radius σ). Thus, the results of previous papers on overlapping disks can be used for a geometrical analysis of the system. The concept of "fluctuating free volume" is compared with free volume theory. Finally, a series of computer experiments on hard disks is analyzed geometrically, especially with respect to the fluid–solid transition.

KEY WORDS: Statistical mechanics; hard disks; intersection of disks; fluctuating free volume; free volume theory; Monte Carlo computer experiments.

1. INTRODUCTION

The overlap of N equal D-dimensional spheres has been considered in Refs. 1, 2. In the present paper, the two-dimensional formulas are used for an analysis of the hard-disk system. The hard disks (diameter σ) cannot overlap, of course. However, the exclusion disks (radius σ) can. The N exclusion disks have the same centers as the N hard disks and are relevant for the hard-disk system.[3] For instance, the centers of disks $1, 2, \ldots, N-1$ cannot be located within exclusion disk N. Properties of overlapping disks and spheres have been studied quite a few years ago for the penetrable-sphere model[4] as well as for the scaled-particle theory.[5] However, approximations had to be used for actual calculations. In the present paper, the three-dimensional diction[2] will be retained (e.g., "free volume" and not "free area") since most of the formulas are valid generally in D dimensions. Throughout the paper, systems with periodic boundary conditions are studied, the volume being V.

[1] Institut für Experimentalphysik der Universität Wien, Boltzmanngasse 5, A-1090 Wien, Austria.

0022-4715/82/1100-0499$03.00/0

The volume of intersection[2] of N D-dimensional spheres $1, 2, \ldots, N$ is abbreviated by $I(1, 2, \ldots, N)$. It is the volume where all N spheres intersect. The corresponding surface is termed $B(1, 2, \ldots, N)$. The following definitions[2] are useful:

$$I_{(j)} \equiv \sum_{1 \leqslant i_1 < \cdots < i_j \leqslant N} I(i_1, \ldots, i_j) = \sum_{M_j} I(i_1, \ldots, i_j), \qquad j \geqslant 0 \quad (1)$$

$$B_{(j)} \equiv \sum_{1 \leqslant i_1 < \cdots < i_j \leqslant N} B(i_1, \ldots, i_j) = \sum_{M_j} B(i_1, \ldots, i_j), \qquad j \geqslant 1 \quad (2)$$

M_j symbolizes the number of nonvanishing contributions to $I_{(j)}$ and thus to $B_{(j)}$. Especially,

$$I_{(0)} = V, \qquad I_{(1)} = NI^*, \qquad B_{(1)} = NB^* \quad (3)$$

I^* and B^* being the volume and surface of a sphere, respectively. Thus, $M_1 = N$ in any case. If one likes to study the structure of the system, the quantities $V_{(k)}$ and $S_{(k)}$ are of advantage. $V_{(k)}$ is the total volume covered by k and only k spheres. $S_{(k)}$ is the total surface of the border between $V_{(k)}$ and $V_{(k+1)}$. Correspondingly, $[S_{(k)} + S_{(k-1)}]$ is the total surface of $V_{(k)}$. The $V_{(k)}, k \geqslant 0$, are disjoint, which is also the case for the $S_{(k)}$. The volume of the system, V, splits up into the $V_{(k)}$:

$$V = \sum_{k \geqslant 0} V_{(k)}, \qquad NB^* = \sum_{k \geqslant 0} S_{(k)} \quad (4)$$

$V_{(0)}$ is the volume which is not covered by any spheres, $S_{(0)}$ is the surface of $V_{(0)}$.

Formal definitions and mathematical relations among the above quantities can be found in Ref. 2. For an easy understanding of the results, the main relations will be given now in the case of exclusion disks:

$$\begin{bmatrix} V_{(0)} \\ V_{(1)} \\ V_{(2)} \\ V_{(3)} \\ V_{(4)} \\ V_{(5)} \end{bmatrix} = \begin{bmatrix} 1 & -1 & 1 & -1 & 1 & -1 \\ 0 & 1 & -2 & 3 & -4 & 5 \\ 0 & 0 & 1 & -3 & 6 & -10 \\ 0 & 0 & 0 & 1 & -4 & 10 \\ 0 & 0 & 0 & 0 & 1 & -5 \\ 0 & 0 & 0 & 0 & 0 & 1 \end{bmatrix} \begin{bmatrix} I_{(0)} \\ I_{(1)} \\ I_{(2)} \\ I_{(3)} \\ I_{(4)} \\ I_{(5)} \end{bmatrix} \quad (5)$$

$$\begin{bmatrix} S_{(0)} \\ S_{(1)} \\ S_{(2)} \\ S_{(3)} \\ S_{(4)} \end{bmatrix} = \begin{bmatrix} 1 & -1 & 1 & -1 & 1 \\ 0 & 1 & -2 & 3 & -4 \\ 0 & 0 & 1 & -3 & 6 \\ 0 & 0 & 0 & 1 & -4 \\ 0 & 0 & 0 & 0 & 1 \end{bmatrix} \begin{bmatrix} B_{(1)} \\ B_{(2)} \\ B_{(3)} \\ B_{(4)} \\ B_{(5)} \end{bmatrix} \quad (6)$$

$V_{(j)} = 0$, $I_{(j)} = 0$ if $j > 5$ and $S_{(k)} = 0$, $B_{(k+1)} = 0$ if $k > 4$ for exclusion disks,[2] which makes the relatively small matrices in (5), (6) possible. For the hard-disk system, all geometrical quantities considered above can be determined analytically[2] for a given configuration of N disks with periodic boundary conditions. For instance, the values $V_{(k)}/V$, $\sum V_{(k)}/V = 1$, give some information about the structure of the system. The computer experimental change of these quantities during the fluid–solid transition will be studied in Section 4.

2. FLUCTUATING FREE VOLUME

Figure 1 shows a possible situation for hard disks at medium fluid density. The vicinity of disk 1 is considered. The exclusion disks are drawn, regions contributing to different $V_{(k)}$ can be distinguished. There is one small (Sm_1) and one large (La_1) region within exclusion disk 1 contributing to $V_{(1)}$. Sm_1 is disconnected from center 1. The probability of occurrence of such a region is very small at any density. Sm_1 can only occur if $r_{12} \approx r_{13} \approx \sigma$, $r_{23} \cong 2\sigma$, and $r_{14} \gtrsim 2\sigma$, see Fig. 1. It is very improbable that all three conditions are fulfilled at the same time, the first condition corresponding to high density, the others to low density.

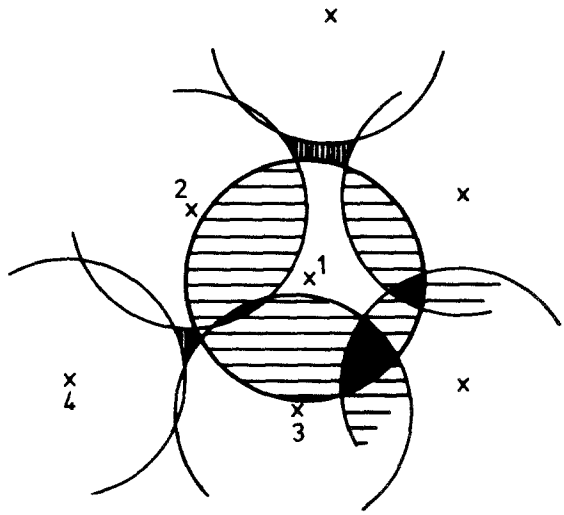

Fig. 1. Configuration of exclusion disks in the vicinity of disk 1. The disk centers are represented by ×, centers 1 to 4 being numbered explicitly. Regions contributing to different $V_{(k)}$ are distinguished as follows if they lie within exclusion disk 1 or are adjacent to it: $k = 0$ (vertically shaded), $k = 1$ (white), $k = 2$ (horizontally shaded), $k = 3$ (black). There are two white regions within exclusion disk 1. They are termed La_1 and Sm_1 in Section 2, each being adjacent to a vertically shaded region.

With neighbors held fixed, disk center 1 can freely move within region La_1 and the adjacent region contributing to $V_{(0)}$. It is the "fluctuating free volume" $v_f(1)$ of disk 1[6] in contrast to the usual (fixed) free volume in free volume theory. However, the formulas of Section 1 only yield the total $V_{(k)}$ and not, e.g., $v_f(1)$. To determine how the $V_{(k)}$ actually split up into separate regions, some kind of pattern recognition would be necessary,[6,7] which is very time-consuming on the computer. In this paper, an approximation will be used to determine $v_f(i)$. If existence of regions Sm_i is ignored and if the density is high enough so that $V_{(0)}$ is negligible, see below, then La_i corresponds to $v_f(i)$. Thus,

$$V_{(1)} \cong \sum_{i=1}^{N} v_f(i) \equiv N\bar{v}_f, \qquad S_{(1)} \cong \sum_{i=1}^{N} s_f(i) \equiv N\bar{s}_f \tag{7}$$

$s_f(i)$ being the surface of the free volume $v_f(i)$. The bar indicates averaging over one configuration. The number of free volumes is trivially N. Generally, N_k shall be the number of regions contributing to $V_{(k)}$. Even without pattern recognition, two of the N_k can be determined from the known M_k, Eq. (1). Neglecting regions Sm_i yields

$$N_1 = M_1 \equiv N \tag{8a}$$

for D-dimensional hard spheres. Moreover,

$$D = 2 : N_5 = M_5 \tag{8b}$$

Equation (8b) follows from the fact that at most five exclusion disks can have a common overlap. Thus, every (nonvanishing) contribution to $I_{(5)}$, Eq. (1), corresponds to a region contributing to $V_{(5)}$. Now, we turn again to the computation of free volume. Equation (7) shows an expression for the mean free volume and its surface, $\bar{v}_f$ and $\bar{s}_f$, valid at high density. A single free volume can also be calculated explicitly as follows. If, e.g., particle 1 is removed from a given configuration, $V_{(0)}$ increases. Using the notation

$$\Delta_i X \equiv X(\text{all particles except } i) - X(\text{all particles}) \tag{9}$$

for any quantity depending on the location of particles it follows for exclusion disks that

$$\Delta_1 V_{(0)} = \sum_{k=0}^{5} (-1)^k \Delta_1 I_{(k)} \tag{10a}$$

compare (5). Only the upper bound $k = 5$ of the sum is specific for the two-dimensional case. Using (1) results in

$$\Delta_1 V_{(0)} = I(1) - \sum_{1<i\leqslant N} I(1,i) + \sum_{1<i<j\leqslant N} I(1,i,j) - \sum_{1<i<j<m\leqslant N} I(1,i,j,m) + \sum_{1<i<j<m<n\leqslant N} I(1,i,j,m,n) \tag{10b}$$

Equivalently,

$$\Delta_1 S_{(0)} = -B(1) + \sum B(1,j) - \sum B(1,i,j) + \sum B(1,i,j,m) - \sum B(1,i,j,m,n) \tag{11}$$

Incidentally, $I(1)$ and $B(1)$ correspond to I^* and B^*, respectively, cf. Eq. (3). Equations (10) and (11) are exact for disks. Now, $\Delta_1 V_{(0)}$ is the contribution of exclusion disk 1 to $V_{(1)}$; cf. Fig. 1. With the assumptions leading to (7), i.e., neglecting Sm_1 and $V_{(0)}$, it follows that $\Delta_1 V_{(0)} = v_f(1)$. If $V_{(0)}$ is small but not negligible, then

$$\Delta_i V_{(0)} \cong v_f(i), \qquad \Delta_i S_{(0)} \cong s_f(i) \tag{12a}$$

$$\left[\Delta_i S_{(0)} / \Delta_i V_{(0)}\right] \cong \left[s_f(i)/v_f(i)\right] \tag{12b}$$

The ratio $s_f(i)/v_f(i)$ will be considered in the following instead of the single quantities $v_f(i)$ and $s_f(i)$. In Section 4, the average difference between the left- and right-hand side of (12b) will be estimated to be less than 0.2% for densities $z \geqslant 0.70$.[2] On the other hand, the hard-disk pressure can be calculated[6] via

$$Z = PV/(NKT) = 1 + \tfrac{1}{4}\sigma\langle s_f/v_f\rangle \tag{13}$$

Combining (12b) with (13), the pressure can be evaluated accurately for the dense fluid and the whole solid. In this density range, the error due to the approximation (12b) is negligible compared with the statistical Monte Carlo error typically being 1%.

As to the meaning of averages, the following diction is used: If we take, e.g., $s_f(i), \bar{s}_f$ means average over $s_f(i)$ within a given configuration. Additional average over all configurations yields $\langle s_f\rangle$. For quantities like $V_{(k)}$, which have a definite value for a given configuration, $\langle V_{(k)}\rangle$ just means average over all configurations.

3. THE CELL MODEL (FREE-VOLUME THEORY)

In the cell model, the disks are located at their lattice positions (triangular lattice). Thus, the free volume is fixed at a given density, $v_f(i) = v_f(j)$. Due to the high symmetry, determination of overlaps is relatively simple. No regions Sm_i occur. For $0 \leqslant z \leqslant 1/4$, the exclusion disks do not overlap at all, and $V_{(0)}$ is singly connected. For $z > 1/4$, nearest neighbors overlap, each disk being confined within the cage of its neighbors. There exist $2N$ small isolated pieces of $V_{(0)}$ if $1/4 < z \leqslant 1/3$.

[2] This may be compared with $z = 1$ for triangular close packing and the phase transition region $z = 0.76$ to $z = 0.80$.[8]

For $z > 1/3$, $V_{(0)}$ vanishes, and overlaps $I(i, j, k) \neq 0$ occur. Starting with $z = 3/4$, next-nearest neighbors also overlap and intersections of four disks occur. At no density, there are overlaps of five exclusion disks. Thus, $N_5 = M_5 = V_{(5)} = S_{(4)} = 0$.

Now we stick to disk 1 again. It is surrounded by six neighbors $2, \ldots, 7$ and six next-nearest neighbors $8, \ldots, 13$. Then,

$$r_{12} = a, \qquad r_{18} = a\sqrt{3}\,, \qquad z = (\sigma/a)^2 = \tfrac{1}{2}\sqrt{3}\,\sigma^2 N/V \tag{14}$$

a being the lattice distance. Furthermore,[2]

$$I^* = \pi\sigma^2, \qquad B^* = 2\pi\sigma, \qquad x_{1j} \equiv r_{1j}/(2\sigma)$$

$$I_{1j} = 2\sigma^2\left[\cos^{-1}(x_{1j}) - x_{1j}\left(1 - x_{1j}^2\right)^{1/2}\right] \tag{15}$$

$$B_{1j} = 4\sigma\cos^{-1}(x_{1j})$$

$I(1, j)$ is termed I_{1j} if it is not zero. Then, $B(1, j)$ is termed B_{1j}. Using the expressions displayed in (14) and (15), Table I shows the results for M_k, $V_{(k)}$ and $S_{(k)}$ in the different density regions. No mean values have to be taken in the cell model (free volume theory) since there are no fluctuations.

A graphical presentation of $V_{(k)}$ as a function of z is shown in Fig. 5, next section, where it is compared with computer experimental results for hard disks. It will be seen that the cell model yields $V_{(k)}$ similar to the "experimental" hard disk system, even in the fluid phase. Strangely enough, the experimental percolation transition from extensive to intensive free volumes[6] ($z = 0.245 + -0.02$) also lies very close to the cell-model value, $z = \frac{1}{4}$. As to the free volume and its surface, the cell-model results are

$$0 \leqslant z \leqslant \tfrac{1}{4} : Nv_f(i) = V_{(1)} + NV_{(0)}\,, \qquad Ns_f(i) = (N-1)S_{(0)} \tag{16a}$$

$$\tfrac{1}{4} < z \leqslant \tfrac{1}{3} : Nv_f(i) = V_{(1)} + 3V_{(0)}\,, \qquad Ns_f(i) = S_{(1)} + 2S_{(0)} \tag{16b}$$

$$\tfrac{1}{3} < z \leqslant 1 : Nv_f(i) = V_{(1)}\,, \qquad Ns_f(i) = S_{(1)} \tag{16c}$$

Apart from a direct calculation, the relations for $s_f(i)$ can also be obtained[2] via $s_f(i) = -(\partial/\partial\sigma)v_f(i)$ and $(\partial/\partial\sigma)V_{(k)} = S_{(k-1)} - S_{(k)}$. Incidentally, the free volume has already been calculated for disks[9] and spheres[10] in the cell model.

Formally, (16b) is also valid for $1/3 < z \leqslant 1$ since $V_{(0)} = S_{(0)} = 0$ then. Relations (16) may be compared with $\Delta_i V_{(0)}$ and $\Delta_i S_{(0)}$, Eq. (12a):

$$\sum_{i=1}^{N} \Delta_i V_{(0)} = V_{(1)}\,, \qquad \sum_{i=1}^{N} \Delta_i S_{(0)} = S_{(1)} - S_{(0)} \tag{17}$$

(17) is generally valid. In the cell model, $\Delta_i V_{(0)}$ and $\Delta_i S_{(0)}$ yield the correct

Table I. M_k/N, $V_{(k)}/N$, and $S_{(k)}/N$ for Exclusion Disks in the Cell Model

	$0 \leqslant z \leqslant 1/4$	$1/4 < z \leqslant 1/3$	$1/3 < z \leqslant 3/4$	$3/4 < z \leqslant 1$
M_1/N	1	1	1	1
M_2/N	0	3	3	6
M_3/N	0	0	2	8
M_4/N	0	0	0	3
M_5/N	0	0	0	0
$V_{(0)}/N$	$(V/N) - I^*$	$(V/N) - I^* + 3I_{12}$	0	0
$V_{(1)}/N$	I^*	$I^* - 6I_{12}$	$3(V/N) - 2I^* + 3I_{12}$	$3(V/N) - 2I^* + 3I_{12}$
$V_{(2)}/N$	0	$3I_{12}$	$-3(V/N) + 3I^* - 6I_{12}$	$-3(V/N) + 3I^* - 6I_{12} + 3I_{18}$
$V_{(3)}/N$	0	0	$(V/N) - I^* + 3I_{12}$	$(V/N) - I^* + 3I_{12} - 6I_{18}$
$V_{(4)}/N$	0	0	0	$3I_{18}$
$V_{(5)}/N$	0	0	0	0
$S_{(0)}/N$	B^*	$B^* - 3B_{12}$	0	0
$S_{(1)}/N$	0	$3B_{12}$	$2B^* - 3B_{12}$	$2B^* - 3B_{12}$
$S_{(2)}/N$	0	0	$-B^* + 3B_{12}$	$-B^* + 3B_{12} - 3B_{18}$
$S_{(3)}/N$	0	0	0	$3B_{18}$
$S_{(4)}/N$	0	0	0	0

$v_f(i)$ and $s_f(i)$ if $z > 1/3$ for hard disks. If $z > 1/4$,

$$\begin{aligned} v_f(i) &= \Delta_i V_{(0)}\left[1 + 3V_{(0)}/V_{(1)}\right] \\ s_f(i) &= \Delta_i S_{(0)}\left[1 + 3S_{(0)}/S_{(1)}\right] \end{aligned} \tag{18}$$

for hard disks in the cell model, cf. (16) and (17). This results in an estimate for the accuracy of pressure obtained via (12b) and (13) in hard-disk computer experiments:

$$\langle s_f/v_f\rangle\langle \Delta S_{(0)}/\Delta V_{(0)}\rangle^{-1} = \left[1 + 3\langle S_{(0)}\rangle/\langle S_{(1)}\rangle\right]\left[1 + 3\langle V_{(0)}\rangle/\langle V_{(1)}\rangle\right]^{-1} \tag{19}$$

This will be used in the next section.

4. COMPUTER EXPERIMENTAL RESULTS

A series of Monte Carlo computer experiments[11] has been accomplished for hard disks (NVT-ensemble). The particle numbers $N = 48$ and $N = 72$ have been investigated over the whole density range, the periodic cell fitting an ideal lattice as usual. In all runs, the first 0.2×10^6 trials were used for equilibration, and will not be considered further. Then, 0.2×10^6 ($z = 0.1$) to 1.6×10^6 ($z = 0.8$) trials were carried out in the fluid range. In the solid region, all runs lasted over 1.0×10^6 trials. The portion of successful trials ("moves") was about 50%. Every 200th trial was analyzed geometrically, giving 1000 to 8000 configurations analyzed for each run. This was a compromise between saving computer time and obtaining reasonable accuracy.

To generate fluid start configurations, 48 (or 72) points were distributed randomly over the cell. Then the system was "compressed" by increasing σ until the closest pair touched. 500 Monte Carlo trials were carried out before increasing σ further. The compression stopped when the desired density was reached. For the solid start configurations, we used an ideal lattice. One of the main purposes of these computer experiments was the study of the phase-transition region, $z = 0.76$ to $z = 0.80$. Only in this region, both fluid and solid start configurations were used. During the computer runs, it was checked, e.g., via the pressure, whether the configurations remained fluid (or solid), see Table II. Fluid start configurations results in fluid systems up to $z = 0.80$, the highest fluid density considered. As to solid start configurations, the system remained solid for $z = 0.775$ and higher densities. At $z = 0.750$, the solid melted quickly. The above statements are true for both particle numbers. Furthermore, the geometrical quantities investigated are not significantly different for $N = 48$ and $N = 72$

Table II. Fluid (F) and Solid (S) States Observed for 72 Disks in the Phase Transition Region. $Z = PV/(NkT)$ together with its Average Standard Deviation for a Single Configuration is Displayed

z	Start	Average	Z	Start	Average	Z
0.725	F	F	8.69 ± 0.94	—	—	—
0.750	F	F	9.60 ± 1.27	S	F	9.70 ± 1.24
0.775	F	F	10.37 ± 1.35	S	S	9.00 ± 1.01
0.800	F	F	11.20 ± 1.41	S	S	10.03 ± 1.11
0.825	—	—	—	S	S	11.35 ± 1.26

in most cases. Thus, $N = 48$ can be considered to be a check of the data, only the results for $N = 72$ being given in Table II and in the following figures.

Since the pressure is an average over particles if expressed via $\langle s_f / v_f \rangle$, Eq. (13), Z makes sense even for a single configuration. Table II shows that the average standard deviation of Z for a single configuration is about the same as the difference in Z between the solid and the fluid. The standard deviation of the average Z was evaluated taking partial averages over trials and turned out to be 0.07 to 0.08 in all cases of the table. If the analyzed trials had been thoroughly independent, the standard deviation would have been 0.01 to 0.02. This comparison confirms that almost no accuracy is lost when analyzing only every 200th configuration since even these configurations are correlated to a high extent.

Now, we turn to the results for the geometrical quantities M_k. Figure 2 shows $\langle M_k \rangle / N$, Eqs. (1), (2), which may be compared with the cell-model values, Table I. Within the accuracy of drawing, $\langle M_5 \rangle / N$ vanishes and the discontinuities between solid and fluid are not observable. From $z = 0.9$ on, $\langle M_k \rangle / N$ is constant. Figure 2 does not reflect the structural difference between the fluid and the solid. A more detailed analysis of $\langle M_5 \rangle / N$, however, yields a remarkable difference; see Fig. 3a. In the cell model, no overlaps of five disks occur; see above. Accordingly, $\langle M_5 \rangle / N$ is almost vanishing in the "experimental" hard-disk solid. In the phase transition region, the fluid shows much more overlaps M_5. This expected result yields a criterion to distinguish geometrically between the two phases.

Figure 4 shows the results for $\langle V_{(k)} \rangle / V$. Now, discontinuities at $z = 0.775$ are detectable for $k = 2, 3$. $\langle V_{(5)} \rangle / V$ is again zero within the accuracy of drawing. For comparison, Fig. 5 displays the values due to the cell model, Section 3. Figures 4 and 5 show a similar pattern which is quite symmetrical around $z = 0.50$ to 0.55. This may be compared with the one-dimensional case[3] where symmetry around $z = 0.50$ occurs. In Fig. 6,

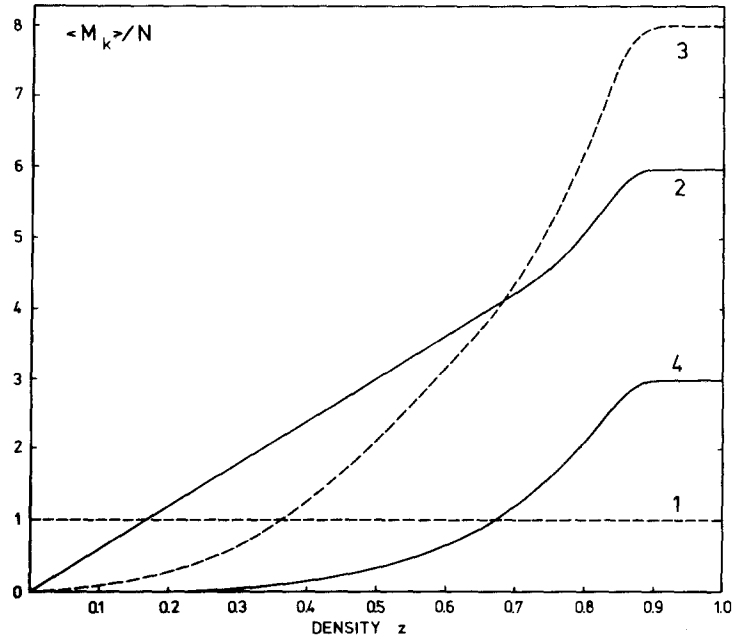

Fig. 2. $\langle M_k \rangle / N$ for hard disks as a function of density z; $k = 1, 2, 3, 4$. The discontinuity between the fluid and solid states at $z = 0.775$ is not visible within the scale chosen.

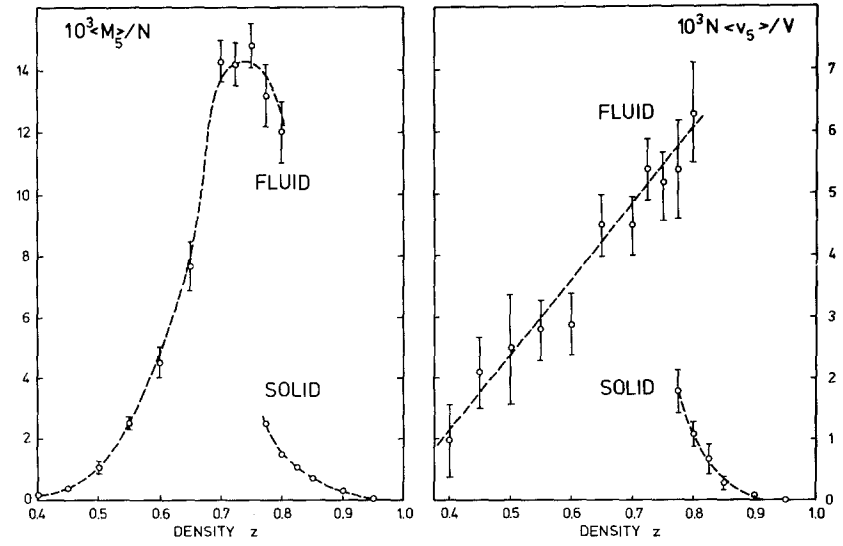

Fig. 3. $\langle M_5 \rangle / N$, Fig. 3a, and $N\langle v_5 \rangle / V$, Fig. 3b, in the phase transition region of hard disks. The standard deviation according to the computer experiments is indicated by error bars.

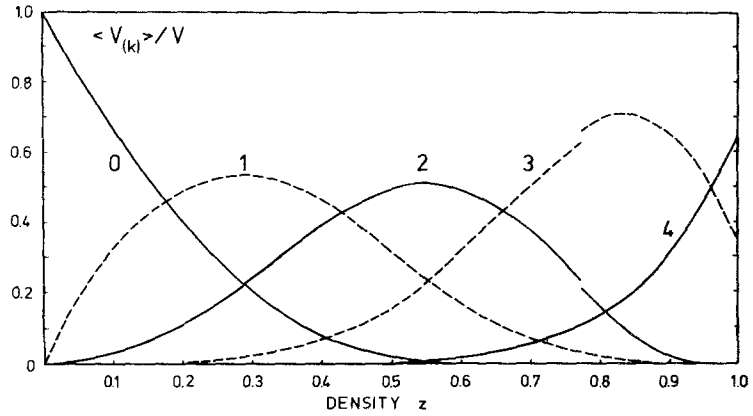

Fig. 4. $\langle V_{(k)}\rangle/V$ as a function of z. According to Eq. (4), $\sum\langle V_{(k)}\rangle/V = 1$. The dashed curves correspond to odd k. For $k = 2$ and 3, the discontinuity between the fluid and solid phases (at $z = 0.775$) can be observed in this figure.

the results concerning $S_{(k)}$ are exhibited. The symmetry is again observable, $\langle S_{(4)}\rangle/(2N\pi\sigma) = \langle S_{(4)}\rangle/(NB^*)$ being zero within the accuracy of drawing. Using an appropriate scale, $V_{(5)}$ and $S_{(4)}$ are qualitatively similar to M_5, Fig. 3a, if the phase transition region is considered. To get further information, we consider

$$\langle v_5\rangle = \langle V_{(5)}\rangle/\langle M_5\rangle = \langle V_{(5)}\rangle/\langle N_5\rangle \tag{20}$$

compare (8b). v_5 is the size of a region contributing to $V_{(5)}$. Figure 3b shows the result. Thus, not only more overlaps of five exclusion disks occur

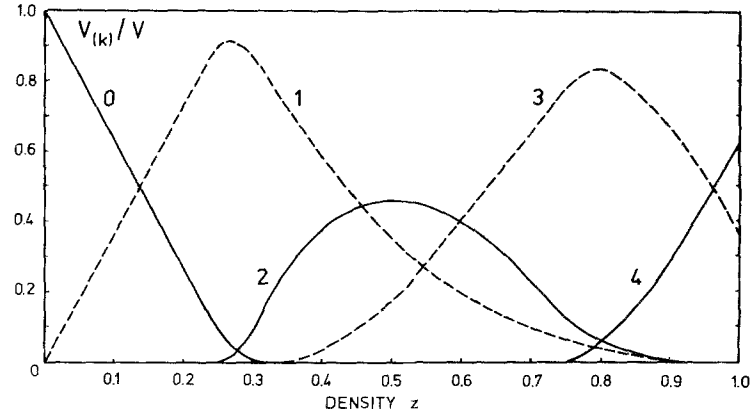

Fig. 5. $V_{(k)}/V$ as a function of z for the cell model. The dashed curves correspond to odd k.

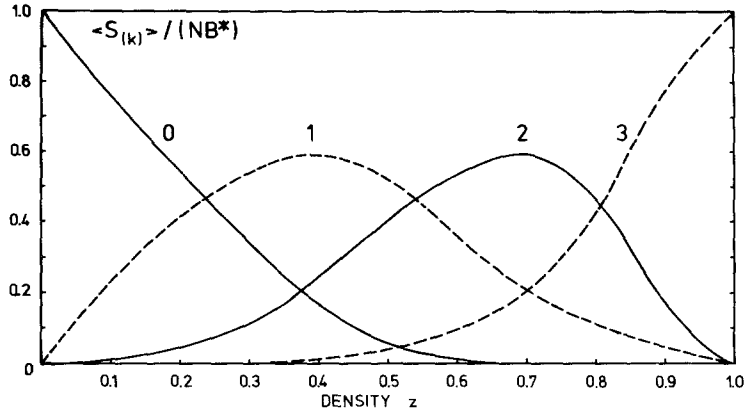

Fig. 6. Computer experimental $\langle S_{(k)}\rangle/(NB^*) = \langle S_{(k)}\rangle/(2N\pi\sigma)$ as a function of z. According to Eq. (4), $\sum\langle S_{(k)}\rangle/(NB^*) = 1$. The fluid–solid discontinuities are too small to be detected in this figure.

Table III. Geometrical Quantities Obtained from Hard-Disk Computer Experiments at $z = 0.775$

	Fluid		Solid			
	$N = 48$	$N = 72$	$N = 48$	$N = 72$	δ_z	δ_P
$\langle M_2\rangle/N$	4.81	4.83	4.77	4.77	$-^a$	$+^a$
$\langle M_3\rangle/N$	5.62	5.66	5.55	5.55	−	+
$\langle M_4\rangle/N$	1.82	1.84	1.78	1.78	−	+
$10^2\langle M_5\rangle/N$	0.87(5)[b]	1.32(9)	0.23	0.25	−	−
$10^4\langle V_{(0)}\rangle/V$	0.056(7)	0.026(6)	0.000(0)	0.000(0)	−	−
$\langle V_{(1)}\rangle/V$	0.034	0.034	0.039	0.038	+	−
$\langle V_{(2)}\rangle/V$	0.224	0.228(3)	0.208	0.209	−	−
$\langle V_{(3)}\rangle/V$	0.637(2)	0.631(3)	0.656	0.655	+	+
$\langle V_{(4)}\rangle/V$	0.105	0.107	0.097	0.098	−	+
$10^2\langle V_{(5)}\rangle/V$	0.004	0.007	0.0004	0.0005	−	−
$N\langle v_5\rangle/V$	0.005	0.005	0.002	0.002	−	−
$10^3\langle S_{(0)}\rangle/(NB^*)$[c]	0.049(4)	0.019(3)	0.000(0)	0.000(0)	−	−
$\langle S_{(1)}\rangle/(NB^*)$	0.134	0.132	0.140	0.140	+	−
$\langle S_{(2)}\rangle/(NB^*)$	0.516	0.514(2)	0.520	0.519	+	−
$\langle S_{(3)}\rangle/(NB^*)$	0.350	0.353	0.340	0.341	−	+
$10^2\langle S_{(4)}\rangle/(NB^*)$	0.037(4)	0.061(7)	0.006	0.007	−	−
$\langle s_4\rangle/B^*$	0.043(7)	0.046(7)	0.027(2)	0.028(2)	−	−

[a] δ is the sign of the difference (solid–fluid). δ_z and δ_P refer to constant z and P, respectively, in the phase transition region.

[b] Generally, the uncertainty of the last digit is ± 1. In any other case, the standard deviation is specified by the number in parentheses.

[c] B^* is equal to $2\pi\sigma$ for exclusion disks, cf. Eq. 15. According to Eq. (4), $\sum\langle S_{(k)}\rangle/(NB^*) = 1$ as well as $\sum\langle V_{(k)}\rangle/V = 1$.

for the fluid (Fig. 3a), but the resulting separate regions are also larger. For a quantitative comparison of the fluid and the solid, Table III shows the values of the geometrical quantities for $N = 48$, 72 at $z = 775$. The uncertainty of these values is ± 1 in the last digit unless stated otherwise. The last but one column indicates if the corresponding value for the solid is larger ("+") of smaller ("−") than for the fluid. The sign is the same for $N = 48$, 72 and may be generalized to any z in the phase transition region. The last column shows the sign of the difference (solid-fluid) not for constant z, but constant pressure in the transition region, where[8]

$$[P_{\text{solid}} = P_{\text{fluid}}] \Rightarrow [z_{\text{solid}} - z_{\text{fluid}} = 0.03 \text{ to } 0.04] \tag{21}$$

In most cases, the difference fluid–solid is small, but significant. The differences between $N = 48$ and 72 are negligible for the solid data. As to the fluid data, the differences are small except for M_5, $V_{(5)}$, and $S_{(4)}$: Interestingly, the mean volume $\langle v_5 \rangle$ of the single regions and their mean surface $\langle s_4 \rangle$,

$$\langle s_4 \rangle = \langle S_{(4)} \rangle / \langle M_5 \rangle = \langle S_{(4)} \rangle / \langle N_5 \rangle \tag{22}$$

coincide for $N = 48$ and 72 within the accuracy. Apart from $V_{(0)}$ and $S_{(0)}$, all fluid values for $N = 48$ differ from $N = 72$ towards the solid data. To interpret this, we remember the fact[12] that computer experiments with high-density fluids may average partly over "solidlike" configurations if N is small. Thus, the results for $N = 72$, $z = 0.775$, seem to be more fluidlike than for $N = 48$. Furthermore, the decrease of $\langle M_5 \rangle / N$ for the fluid in the phase transition region, Fig. 3a, may be interpreted as an artificial consequence of the boundary conditions. Finally, it shall be mentioned that the differences between the fluid and solid $\langle V_{(k)} \rangle / V$ are not in agreement with the predictions of Speedy.[3]

Now, it can also be estimated at which density the calculation of pressure via (13) becomes accurate when approximation (12b) is used. The quantities $S_{(0)}, S_{(1)}, V_{(0)}, V_{(1)}$ necessary to utilize (19) are known due to the described computer experiments. Table IV shows that the influence of using $\Delta_i V_{(0)}$ and $\Delta_i S_{(0)}$ instead of $v_f(i)$ and $s_f(i)$ becomes negligible at $z \cong 0.70$ if an inaccuracy of 1% is assumed for the data. Thus, the pressure of the high-density fluid and the whole solid can be determined via (12b) and (13), in the following, called method Δ. The usual Monte Carlo method to determine the hard-disk pressure needs the radial distribution function at contact, $g(\sigma)$. Due to the necessary extrapolation, this method ("g") in-

Table IV. $Q = \langle s_f / v_f \rangle \langle \Delta S_{(0)} / \Delta V_{(0)} \rangle^{-1}$, **Estimated via Eq. (19)**

z	0.55	0.60	0.65	0.70	0.75
Q	1.062	1.030	1.011	1.002	1.001

cludes an additional uncertainty. Both methods have been compared in an additional investigation. For this purpose, Monte Carlo runs have been carried out for $N = 71$, 72, and 73 at $z = 1/1.4 = 0.714$. For each particle number, three box shapes have been investigated, length ratio $\frac{1}{4}3^{3/2} = 1.299$ of the rectangular cell corresponding to the usual boundary conditions for 72 disks. Each run consisted of 6×10^5 trials, every 200th trial being analyzed. Table V shows the results for compressibility factor $Z = PV/(NkT)$, the accuracy being ± 0.1. For a detailed analysis of the standard deviation, see below. The results of the two methods do not differ systematically, cf. the last line of Table V. This is no surprise because approximation (12b), estimated via Eq. (19), reduces Z only by 0.01 compared with the correct Eq. (13). Thus, both methods (Δ and g) are considered to yield unbiased estimates of the same Z for a given computer run. Then the differences between Z_Δ and Z_g shown in Table V result from the uncertainty of the extrapolated $g(\sigma)$. This can be verified by a study of the variances Var. For method Δ,, the variance Var_Δ of Z_Δ in a computer run comes from the "true" fluctuations during the run. For method g, the additional variance Var_E due to the uncertainty of the extrapolation is assumed to be independent of the above-mentioned fluctuations. Then, the law of error propagation yields

$$\mathrm{Var}_g = \mathrm{Var}_\Delta + \mathrm{Var}_E \tag{23}$$

Table V. Compressibility Factor $Z = PV/(NkT)$ for Various N and Length Ratios l of the Periodic Cell. The Results Z_Δ and Z_g are Compared, Methods Δ and g Being Described in the Text.

N	l	Z_Δ	Z_g
71	1.05	8.31[a]	8.31
71	1.299	8.31	8.37
71	1.60	8.20	8.19
72	1.05	8.25	8.23
72	1.299	8.26	8.17
72	1.60	8.04	8.01
73	1.05	8.20	8.19
73	1.299	8.12	8.07
73	1.60	8.09	8.11
Mean		8.20	8.18

[a] The standard deviation is 0.1 in all cases.

$\mathrm{Var}_g = 0.010$ and $\mathrm{Var}_\Delta = 0.007$ have been obtained in the computer runs. Thus, $\mathrm{Var}_E = 0.003$, which yields ± 0.05 for the corresponding uncertainty of Z. This is confirmed by the root-mean-square deviation of the nine pairs (Z_Δ, Z_g) of Table V, which is 0.04. From the above considerations it follows that at high-density method Δ is an alternative to the direct determination of $v_f(i)$ and $s_f(i)$ suggested by Hoover *et al.*[6] Geometrical analysis of the hard-disk system as described throughout the paper yields Z_Δ automatically without additional consumption of computer time. An analogous analysis for the hard-sphere system would also be possible in principle.[2] However, the analytical formula for the intersection of four spheres is lacking up to now. We will try to calculate this overlap in order to complete our investigations on hard-sphere systems.

ACKNOWLEDGMENT

The authors are very grateful to Professor P. Weinzierl for continuous interest in this work.

REFERENCES

1. K. W. Kratky, *J. Phys. A* **11**:1017 (1978).
2. K. W. Kratky, *J. Stat. Phys.* **25**:619 (1981).
3. R. J. Speedy, *J. Chem. Soc. Faraday Trans. II* **76**:693 (1980).
4. B. Widom, *J. Chem. Phys.* **54**:3950 (1971).
5. H. Reiss, *Adv. Chem. Phys.* **9**:1 (1965).
6. W. G. Hoover, N. E. Hoover, and K. Hanson, *J. Chem. Phys.* **70**:1837 (1979).
7. J. A. Zollweg, *J. Chem. Phys.* **72**:6712 (1980).
8. W. G. Hoover and F. H. Ree, *J. Chem. Phys.* **49**:3609 (1968).
9. R. D. Larsen, *J. Chem. Phys.* **61**: 1591 (1974).
10. R. J. Buehler, R. H. Wentorf, Jr., J. O. Hirschfelder, and C. F. Curtiss, *J. Chem. Phys.* **19**:61 (1951).
11. H. Drexler, thesis, Vienna 1981.
12. W. W. Wood, LACL Report LA-2827 (1963).